

ARTICLES

Hydrogen-Bond Formation between Isoindolo[2,1-*a*]indol-6-one and Aliphatic Alcohols in *n*-Hexane

Attila Demeter* and Tibor Bérces

Institute of Structural Chemistry, Chemical Research Center, Hungarian Academy of Sciences, 1025 Budapest, Pusztaszeri u. 59-67, Hungary

Received: October 4, 2004; In Final Form: January 11, 2005

The spectroscopic, kinetic, and equilibrium properties of isoindolo[2,1-*a*]indol-6-one (**I**) were studied in *n*-hexane in the presence and absence of alcohols (**X**). Hydrogen-bonded-complex formation was found to occur between the alcohol and the ground state as well as the excited state of the **I** molecule. The spectra of **I** and its singly complexed derivative (**IX**) are similar; however, that of **IX** is red shifted. The extent of red shift increases with the hydrogen-bonding ability of the alcohol. Equilibrium constant measurements were made to determine the hydrogen-bond basicity (β_2^H) for **I** and the singlet excited $^1\mathbf{I}$. The β_2^H value for $^1\mathbf{I}$ is found to be about twice that of the ground-state **I**. Time-resolved fluorescence decay measurements indicate that the reaction of singlet excited **I** with fluorinated alcohols is diffusion controlled, while the rate of complexation with nonfluorinated (weaker hydrogen bonding) aliphatic alcohols depends on the Gibbs energy change in the complexation reaction. The quantitative correlation between the rate coefficient of complexation of $^1\mathbf{I}$ with alcohols and the Gibbs energy change in the complexation process allowed us to estimate the rate coefficient for the complexation of the ground-state **I** with alcohols. The formation of the singlet excited hydrogen-bonded complex is irreversible; $^1\mathbf{IX}$ disappears in a first order and an alcohol induced second order reaction. The first order decay is predominantly due to internal conversion to the ground state, the rate of which depends on the ionization energy of the complexing alcohol.

Introduction

As a continuation of the study of the photophysics of heterocyclic aromatic compounds,^{1,2} in this paper, we deal with the kinetic and equilibrium properties of photoinitiated processes of isoindolo[2,1-*a*]indol-6-one (**I**, Figure 1) in the presence of alcohols (i.e., isopropanol (IPA), ethanol (ETOH), methanol (MET), difluoroethanol (DFE), trifluoroethanol (TFE), hexafluoro-2-propanol (HFIP), and perfluoro-*tert*-butyl alcohol (PFTB)). Particular emphasis is placed on the understanding of the influence of the strength of the hydrogen bond on the rate of complex formation and depopulation.

Indole derivatives are common in nature.³ **I** contains the amide structural unit which occurs in many organic molecules of biological importance.³ The –CON– moiety in **I** and related compounds may lead to complex formation in an environment containing hydrogen-bond donors. Hydrogen bonding is known to influence the physicochemical properties, including the photophysics, of many heteroaromatic compounds.⁴ Considerable knowledge has accumulated on the equilibrium properties of hydrogen-bonded systems;^{5,6} however, much less is known on the kinetics of these processes.^{7,8} In a previous study,⁹ we investigated the spectroscopy and thermodynamics of the hydrogen-bond formation of *N*-(2,6-dimethylphenyl)-2,3-naphthalimide (DMPN) with fluorinated alcohols in *n*-hexane.

* To whom correspondence should be addressed. E-mail: demeter@chemres.hu.

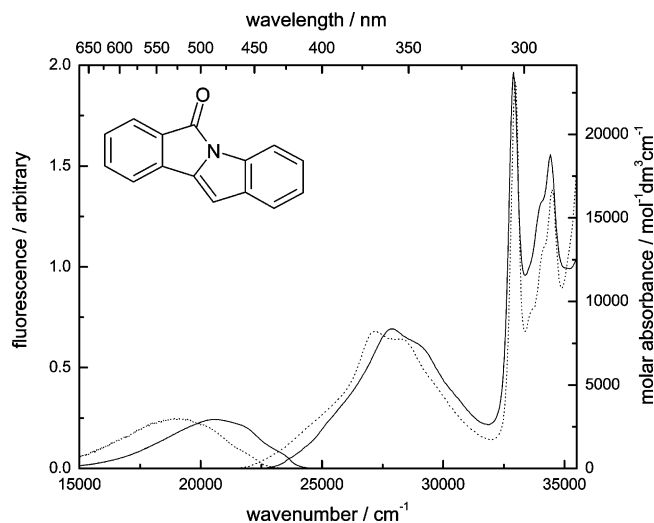


Figure 1. Absorption and fluorescence spectra of **I** (full line) and of the complex of **I** with HFIP (dotted line) in *n*-hexane.

Complexation was found to occur both in the ground and excited singlet states. Besides other properties, the hydrogen-bond basicity (related to the hydrogen-bonding equilibrium constant) was determined for these species, including the basicity of the electronically excited molecule.

Experimental Section

The absorption spectra were recorded on a thermoregulated Unicam UV500 spectrophotometer with a resolution typically of 0.5 nm. When necessary, correction was made for dilution caused by the addition of alcohol and for density change due to variation in temperature. The corrected fluorescence spectra were obtained on a Jobin-Yvon Fluoromax photon-counting spectrofluorimeter with 0.5 nm resolution. The excitation wavelength was around 362 nm, the isobestic point of the absorption spectra. Room temperature fluorescence quantum yields were determined relative to that of quinine sulfate ($\Phi_f = 0.546$).¹⁰ Time-resolved fluorescence measurements were made by the single-photon-counting technique with Picoquant diode laser excitation at 404 nm. Emission was detected perpendicular to the excitation line by a Hamamatsu H5783 photomultiplier using an Applied Photophysics monochromator. The signals were collected on a Picoquant Timeharp 100 computer card with a 36 ps channel width.⁸ The typical half-width of the detected pulse was ~ 570 ps. Transient absorption measurements were made using the 308 nm (XeCl) light pulses from a Lambda Physics EMG 101 excimer laser. The signals were recorded on an optical line (Xe lamp, thermostated sample, Applied Photophysics monochromator, RCA 928 photomultiplier, and Hitachi VC6041 digital oscilloscope) mounted perpendicular to the excitation. The intersystem crossing yields were determined by the energy transfer method with perylene as the energy acceptor.² These measurements were made relative to the triplet yield of *N*-methyl-1,8-naphthalimide in *n*-hexane (${}^3\Phi = 0.95$).¹¹

I was prepared by intramolecular photoreduction of *N*-(2-methylphenyl)-phthalimide, as described in the literature.¹² The crude compound was purified by column chromatography and crystallization from *n*-hexane–chloroform mixture. Further purification was carried out by preparative thin-layer chromatography (Merck PLC silica gel) with *n*-hexane–ethyl acetate solvent mixture as the eluent. Methanol and carbon tetrachloride for UV spectroscopy were obtained from Fluka. The *n*-hexane for spectroscopy, ethanol, and 2-propanol were of Merck Uvasol quality and were used as received. Fluorinated alcohols were purchased from Fluorochem Limited (except 2,2-difluoroethanol which was delivered by Apollo Scientific LTD) and were used without further purification.

Results and Discussion

1. Absorption and Fluorescence Spectra of I. The absorption and fluorescence spectra of **I** show mirror symmetry (Figure 1). As seen from the long-wavelength region of the absorption spectrum, the lowest energy band is probably of charge transfer character. This is in agreement with the yellow color of the compound and with the practically structureless absorption band. Hückel level and AM-1 calculations indicate that the $S_1 \leftarrow S_0$ transition corresponds to electron transfer from the highest occupied molecular orbital (HOMO) to the lowest unoccupied molecular orbital (LUMO). There is no other singlet state with comparable low energy. In addition, the calculations suggest that S_1 is a $\pi\pi^*$ state formed by electron transition from the aromatic moiety to the carbonyl group. The change in the dipole moment is expected to be small, in accordance with the experimental observations.¹³

The fluorescence quantum yield of **I**, measured in *n*-hexane against quinine sulfate, is $\Phi_f = 0.51 \pm 0.04$, which is significantly lower than the value ($\Phi_f = 0.9$) reported by Disanayaka and Weedon¹³ from measurements made in *n*-hexane against indole (for which the quantum yield is not given

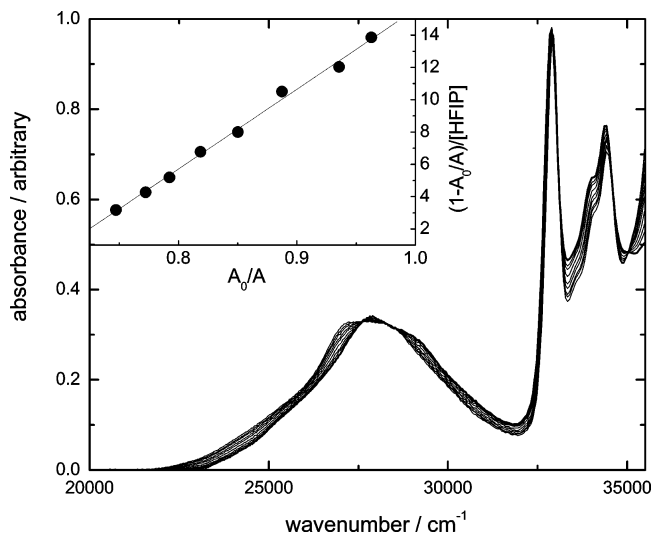


Figure 2. Absorption spectra of **I** (4.18×10^{-5} mol dm⁻³) with and without HFIP additives in *n*-hexane. (At 25 000 cm⁻¹, the increasing absorbances correspond to 0, 0.0027, 0.0054, 0.011, 0.019, 0.027, 0.040, 0.053, and 0.080 mol dm⁻³ HFIP concentrations.) Inset: linearized plot (in accordance with eq 2) of the 400 nm absorbance results.

in the cited literature). A relatively low triplet yield of $\Phi_{isc} = 0.080 \pm 0.01$ was determined, and consequently, $\Phi_{ic} = 0.41 \pm 0.05$ was obtained. The lifetime of the singlet excited state is found to be long, $\tau_0 = 23.2 \pm 0.2$ ns.

2. Influence of Alcoholic Additives on the Fluorescence and Absorption Spectra. The effect of alcoholic additives on the **I** spectrum has been investigated in *n*-hexane with methanol and four fluorinated alcohols. The results obtained with HFIP are given in Figure 2. The addition of alcohol caused a slight red shift of the spectrum; a more significant shift is observed at the longer wavelengths. The shift is explained as a consequence of the formation of a hydrogen-bonded complex (**IX**) from the interaction of **I** with the alcohol (**X**):



If **X** is in large excess of **I**, the change in absorbance can be analyzed by the equation derived by Mataga et al.:¹⁴

$$\frac{1 - \frac{A_0}{A}}{[\mathbf{X}]_0} = -K_1 + K_1 \frac{\epsilon_{\mathbf{IX}}}{\epsilon_1} \frac{A_0}{A} \quad (2)$$

where K_1 is the equilibrium constant of reaction 1, A_0 and A are the absorbances at a given wavelength in the absence and presence of alcohol, respectively, while ϵ_1 and $\epsilon_{\mathbf{IX}}$ are the molar absorption coefficients of **I** and **IX**, respectively. For the **I**–HFIP–*n*-hexane system, the plot of absorbances, according to eq 2, is shown in the inset of Figure 2. The good straight line of the plot supports the singly complexed nature of the new absorbing species. From the intercept of the plot, the equilibrium constants can be directly obtained. These results are given for different alcohols in the third column of Table 1.

The temperature dependence of the equilibrium constant for complex formation was studied for the **I**–HFIP–*n*-hexane system in the temperature range 15–60 °C. A reaction enthalpy of $\Delta H_1^\circ = -5.7 \pm 0.3$ kcal mol⁻¹ and a reaction entropy of $\Delta S_1^\circ = -12.05 \pm 0.80$ cal mol⁻¹ K⁻¹ were derived from the van't Hoff plot.

Knowledge of the K_1 equilibrium constant allows us to derive the spectrum of the complexed species (**IX**). Using the absorp-

TABLE 1: Thermodynamic, Spectroscopic, and Kinetic Data for the I–Alcohol–*n*-Hexane System at Room Temperature

| alcohol | α_2^H | K_1^a (mol ⁻¹ dm ³) | Δ^1E^a (kcal mol ⁻¹) | ΔG_1° (kcal mol ⁻¹) | ΔG_4° ^b (kcal mol ⁻¹) | k_4^a (mol ⁻¹ dm ³ s ⁻¹) | k_9^a (10 ⁸ s ⁻¹) | k_{10}^a (mol ⁻¹ dm ³ s ⁻¹) | IE ^c (eV) |
|---------|--------------|---|--|---|--|---|---|--|-------------------------|
| PFTB | 0.88 | 98 ± 5 | -3.8 ± 0.1 | -2.71 ± 0.03 | -6.6 | (1.33 ± 0.02) × 10 ¹⁰ | 2.3 ± 0.8 | (1.1 ± 0.2) × 10 ¹⁰ | 12.25 |
| HFIP | 0.77 | 35 ± 4 | -3.43 ± 0.1 | -2.10 ± 0.07 | -5.6 | (1.24 ± 0.10) × 10 ¹⁰ | 1.7 ± 0.8 | (1.2 ± 0.2) × 10 ¹⁰ | 11.94 |
| TFE | 0.57 | 7.9 ± 1.5 | -2.7 ± 0.1 | -1.22 ± 0.11 | -3.8 | (1.16 ± 0.07) × 10 ¹⁰ | 2.0 ± 0.8 | (1.5 ± 0.3) × 10 ¹⁰ | 11.49 |
| DFE | 0.53 | 5.6 ± 1.5 | -2.1 ± 0.2 | -1.02 ± 0.16 | -3.3 | (0.54 ± 0.04) × 10 ¹⁰ | 3.8 ± 0.5 | (0.54 ± 0.04) × 10 ¹⁰ | |
| MET | 0.43 | 3.0 ± 1.5 | -1.7 ± 0.2 | -0.65 ± 0.32 | -2.5 | (0.18 ± 0.01) × 10 ¹⁰ | 7.9 ± 0.8 | (0.17 ± 0.03) × 10 ¹⁰ | 10.85 |
| ETOH | 0.37 | | | | -1.9 | (0.18 ± 0.01) × 10 ¹⁰ | 9.7 ± 1.0 | (0.16 ± 0.05) × 10 ¹⁰ | 10.40 |
| IPA | 0.33 | | | | -1.6 | (0.095 ± 0.006) × 10 ¹⁰ | 22 ± 3 | | 10.29 |

^a The given uncertainties are the statistical errors at the 2 σ level. ^b Derived by means of eq 6 using $\beta_2^H(\mathbf{I})$. ^c Reference 15.

tion spectrum of **I**, as well as the spectrum of **I** measured in the presence of an adequate concentration of the alcohol, the absorption spectrum of the complexed species (**IX**) is obtained by a procedure similar to that previously used for similar cases.⁹ The spectrum of the hydrogen-bonded complex between **I** and HFIP is presented as an example in Figure 1. The absorption spectra of **I** and **IX** are similar; however, that of **IX** is red shifted relative to **I** by ~5–10 nm. The extent of red shift increases with the hydrogen-bonding ability of the alcohol. The molar absorption coefficient at the maximum is similar for the uncomplexed and complexed species.

In addition to the absorption, the fluorescence spectra for the complexed species were also derived. This derivation is complicated by the fact that the singlet excited **IX** species can be formed via two different routes, that is, by the excitation of the ground-state **IX**



and by the complexation of singlet excited **I**.



To determine the fluorescence spectrum of the complexed species (**IX**), fluorescence spectra were determined for **I** without additive and for samples with various alcohol concentrations. By means of the known K_1 equilibrium constant, the α percentage of the uncomplexed species was calculated which corresponds to the fraction of the light intensity absorbed by **I**. (Note that excitation is at the isobestic point of the absorption spectra.) Using the experimentally determined decay parameters of the uncomplexed species **I** in the presence and absence of alcohol (τ_1 and τ_0 , respectively), one can calculate the fluorescence intensity of **IX** at a given wavelength:

$$i_f(\mathbf{IX}) = \left\{ i_f(\text{sample}) - i_f(\mathbf{I})\alpha \frac{\tau_1}{\tau_0} \right\} / \left(1 - \alpha \frac{\tau_1}{\tau_0} \right) \quad (5)$$

where $i_f(\mathbf{I})$, $i_f(\mathbf{IX})$, and $i_f(\text{sample})$ are the fluorescence intensities emitted by **I**, **IX**, and the sample containing alcohol, respectively. The fluorescence spectrum of **I** complexed with HFIP is shown, as an example, in Figure 1. Both the uncomplexed and the complexed species show almost structureless fluorescence. The spectrum of **IX** is red shifted compared to the uncomplexed one. The extent of the shift is ~40 nm with HFIP and PFTB complexing agents and decreases with decreasing hydrogen-bond-forming ability of the alcohol. As compared to the significant fluorescence quantum yield of **I** ($\Phi_f = 0.51$), the fluorescence yields of the complexed species are small. The value slightly depends on the applied alcohol and decreases significantly with increasing alcohol concentration. (For ex-

ample, with HFIP, the yield decreases from 0.03 to 0.01 when the concentration of alcohol increases from 0.004 to 0.08 mol dm⁻³.)

The spectrum in the region of the first absorption band is practically structureless; therefore, the following procedure has been adopted¹⁶ in the determination of the singlet energy: the scale of the fluorescence spectrum relative to the absorption one is chosen in such a way that it ensures mirror symmetry in the low energy range of the absorption spectrum. Singlet energy is obtained as the energy of the crossing point of the two spectra. In this way, the $\Delta^1E = {}^1E(\mathbf{IX}) - {}^1E(\mathbf{I})$ differences in the singlet energy of the complexed and uncomplexed species (given in the fourth column of Table 1) are obtained. Note that the singlet energy for **I** is ${}^1E = 67.6$ kcal mol⁻¹ (23 650 cm⁻¹).

3. Hydrogen-Bond Basicity of **I and **I**.** Abraham⁶ has expressed log K of a complexation process, in carbon tetrachloride at 298 K, as a function of the product of the solute hydrogen-bond acidity (α_2^H) and the hydrogen-bond basicity (β_2^H):

$$\log K = 7.354\alpha_2^H\beta_2^H - 1.094 \quad (6)$$

The equilibrium constant ($K_1 = 19 \pm 3$ mol⁻¹ dm³) measured for the **I**–HFIP system in carbon tetrachloride and the $\alpha_2^H(\text{HFIP}) = 0.77$ hydrogen-bond acidity, from the database of Abraham,⁶ are used to derive from eq 6 the hydrogen-bond basicity $\beta_2^H(\mathbf{I}) = 0.42$.

More detailed equilibrium constant measurements were carried out in *n*-hexane solvent, where complexation with five different alcohols was studied. Interpretation of these results by means of eq 6 requires α_2^H values determined in *n*-hexane which are not available. However, all known experimental results show that the α_2^H scale is practically independent of the solvent;^{6b,9} thus, α_2^H values given in the database of Abraham⁶ will be used below.

In Figure 3, the log K_1 values, measured in *n*-hexane, are plotted against α_2^H . The intercept of the straight line is -1.02 ± 0.10 which agrees within the limits of experimental error with the -1.094 value reported by Abraham^{6a} from numerous measurements made in carbon tetrachloride. The slope of the plot is 3.40 ± 0.17 . In our previous publication,⁹ it was shown that the slope parameter of eq 6 is 14% higher for *n*-hexane than that for carbon tetrachloride, that is, 8.383 instead of 7.354. With this higher parameter and the experimentally determined slope 3.40, a hydrogen-bond basicity of $\beta_2^H(\mathbf{I}) = 0.41 \pm 0.02$ is obtained. This agrees closely with the hydrogen-bond basicity of **I** derived in carbon tetrachloride.

In a previous study of the photophysics of the DMPN–fluorinated alcohol–*n*-hexane system, we showed⁹ that a linear relationship exists between the Δ^1E difference of the singlet excitation energy of the complexed and uncomplexed species on one hand and the Gibbs energy change in the ground-state complexation reaction on the other hand. The equation rewritten

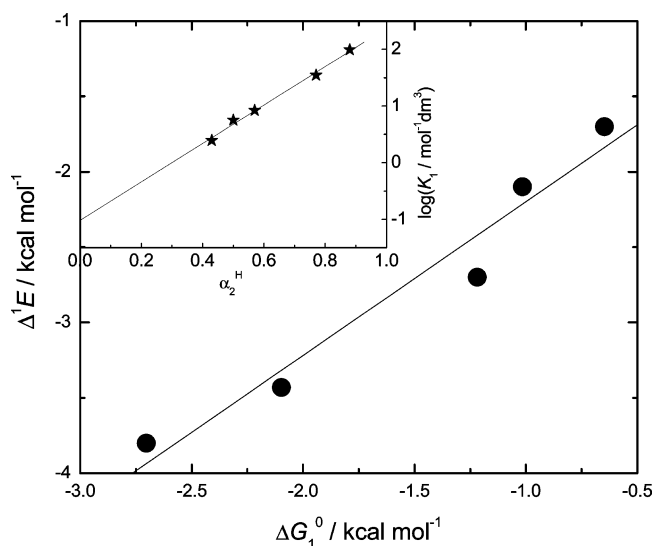


Figure 3. Singlet excitation energy difference of complexed and uncomplexed species (Δ^1E) as a function of Gibbs energy change of complex formation in the **I**–alcohol–*n*-hexane system at 25 °C. The sequence of alcohols from right to left is MET, DFE, TFE, HFIP, and PFTB. Inset: plot (in accordance with eq 6) of the logarithm of the equilibrium constant for complexation as a function of hydrogen-bond acidity in *n*-hexane.

for the **I**–alcohol–*n*-hexane system is

$$\Delta^1E = {}^1E_{\text{IX}} - {}^1E_{\text{I}} = \frac{\beta_2^{\text{H}}(\text{I}) - \beta_2^{\text{H}}(\text{I})}{\beta_2^{\text{H}}(\text{I})} \Delta G_1^0 - RT \frac{\beta_2^{\text{H}}(\text{I}) - \beta_2^{\text{H}}(\text{I})}{\beta_2^{\text{H}}(\text{I})} C_1 \quad (7)$$

where $C_1 = 2.303 \times 1.094$ which corresponds to the intercept parameter in eq 6. The plot of Δ^1E versus $\Delta G_1^0 = -RT \ln K_1$ for the **I**–fluorinated alcohol–*n*-hexane system is shown in Figure 3 to give a reasonably good straight line. With the known ground-state $\beta_2^{\text{H}}(\text{I})$ value, the hydrogen-bond basicity of **I** can be obtained using either the slope or the intercept of the plot. The β_2^{H} values, derived from the slope and intercept, are in good agreement and yield an average of $\beta_2^{\text{H}}(\text{I}) = 0.81 \pm 0.04$. This is almost double the hydrogen-bond basicity of the ground-state species and shows that the amide group in **I** is an excellent hydrogen-bond acceptor. The $\beta_2^{\text{H}}(\text{I})$ value obtained for a heterocyclic amide can be compared with the $\beta_2^{\text{H}}(\text{DMPH}) = 0.64$ value determined previously for an imide in the excited state.⁹

Knowledge of the basicity of **I** in the excited state allows us to calculate the equilibrium constant of complexation of **I** with various alcohols (by means of eq 6) and to determine the ΔG_4^0 Gibbs energy change for the complexation processes (which are given in the sixth column of Table 1).

4. Determination of the Rate Coefficients of Excited-State Reactions of **I and **IX**.** Time-resolved fluorescence decay measurements were made in order to study the mechanism and kinetics of the singlet excited **IX** formation and decay. Excitation was at 404 nm, and 520 ± 20 nm was selected as the monitoring wavelength for the **IX** species. (At this wavelength, **IX** is the major contributor to the emission.) Without added alcohol, single-exponential decay was found, while, in the presence of alcohol, two-exponential kinetics was observed:

$$i_f = A_1 \exp(-t/\tau_1) + A_2 \exp(-t/\tau_2) \quad (8)$$

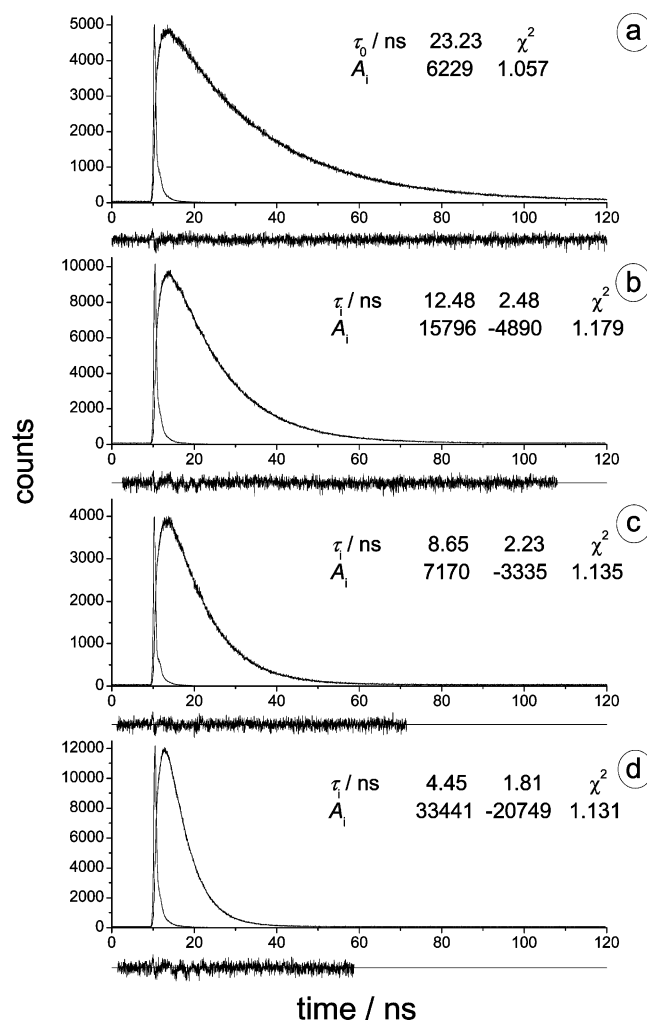


Figure 4. Fluorescence response functions of $5.3 \times 10^{-5} \text{ mol dm}^{-3}$ **I** (a) and **I** with 0.0032 mol dm⁻³ (b), 0.0126 mol dm⁻³ (c), and 0.0316 mol dm⁻³ (d) DFE in *n*-hexane at 25 °C.

In this equation, the preexponential factors and decay parameters A_2 , τ_2^{-1} and A_1 , τ_1^{-1} refer to the short-lived and long-lived fluorescence decay components, respectively. In Figure 4, the fluorescence decay curves of $5.3 \times 10^{-5} \text{ mol dm}^{-3}$ **I** observed in the absence and presence of various amounts of DFE in *n*-hexane are presented. Both the τ_1^{-1} and τ_2^{-1} decay parameters depend on the alcohol concentration for all alcohols investigated. In the case of DFE additive, the preexponential factor A_2 is negative, and the A_2/A_1 ratio is found to decrease from -0.31 to -0.69 with an increase in the alcohol concentration from 0.003 to 0.047 mol dm⁻³. The negative value for A_2 indicates that the emitting **IX** is mainly formed via reaction 4 by the complexation of **I**. Moreover, a A_2/A_1 ratio greater than -1 may arise from two effects: (i) additional direct formation of **IX** by light absorption of the ground-state complex (**IX**) via reaction 3 and/or (ii) the contribution of **I** to the fluorescence at the monitoring wavelength. Similar observations regarding the A_2/A_1 ratio were made also in experiments with other alcohols such as IPA, ETOH, and MET. However, in the cases of the best hydrogen-bond-donating alcohols (TFE, HFIP, and PFTB), positive A_2/A_1 ratios were found, which indicates that in these cases a dominant part of the emitting singlet excited **IX** is formed via reaction 3 from the ground-state complex by light absorption.

The Gibbs energy change in the complexation of **I** is between -1.6 and $-6.6 \text{ kcal mol}^{-1}$ (ΔH_4^0 is approximately between -5.2 and $-10.2 \text{ kcal mol}^{-1}$). Therefore, the complexation

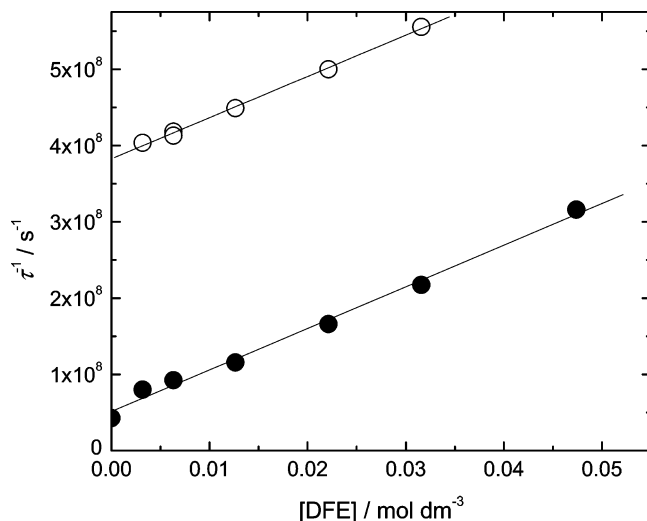
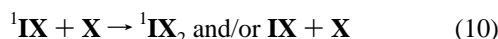


Figure 5. The dependence of τ_1^{-1} (●) and τ_2^{-1} (○) decay parameters on DFE concentration.

process is expected to be practically irreversible. As a test of this conclusion, an experiment was made with HFIP in which a monitoring wavelength of 425 nm was used where only the uncomplexed species emits. Using this monitoring wavelength, a single-exponential decay was observed with a lifetime closely agreeing with the long-lived component of the double-exponential fluorescence decay.

Assuming irreversible complexation processes and taking into account the dependence of the decay parameters on alcohol concentration (see Figure 4), it follows that the longer lifetime (τ_1) can be associated with the complexation of ${}^1\mathbf{I}$ (reaction 4 in the forward direction), while the shorter lifetime (τ_2) is related to the reactions of ${}^1\mathbf{IX}$ via processes 9 and 10:



Reaction 10 is either a complexation reaction or a quenching process. A comparison of the fluorescence spectra of ${}^1\mathbf{IX}$ determined at various alcohol concentrations showed no definite sign of the formation of the doubly complexed singlet species (${}^1\mathbf{IX}_2$).

The dependence of the decay parameters on the DFE concentration is presented in Figure 5. Good straight lines are obtained with DFE and with other alcohols, too. Thus,

$$\tau_1^{-1} = k_0 + k_4[\mathbf{X}] \quad (11)$$

and

$$\tau_2^{-1} = k_9 + k_{10}[\mathbf{X}] \quad (12)$$

The rate parameter $k_0 = \tau_0^{-1}$ is $4.31 \times 10^7 \text{ s}^{-1}$; moreover, the rate coefficients obtained for k_4 , k_9 , and k_{10} are summarized in Table 1. When considering the reliability of the kinetic parameters given in Table 1, one has to take into account the way in which these parameters are derived. At the wavelengths of the measurements (i.e., at 520 nm or above), the emission spectra of ${}^1\mathbf{I}$ and ${}^1\mathbf{IX}$ overlap. The most reliable rate coefficient is k_4 because it is derived from the dominant decay parameter τ_1^{-1} , while k_9 and k_{10} are obtained from τ_2^{-1} which corresponds to the weaker ${}^1\mathbf{IX}$ emission (see eqs 11 and 12). These

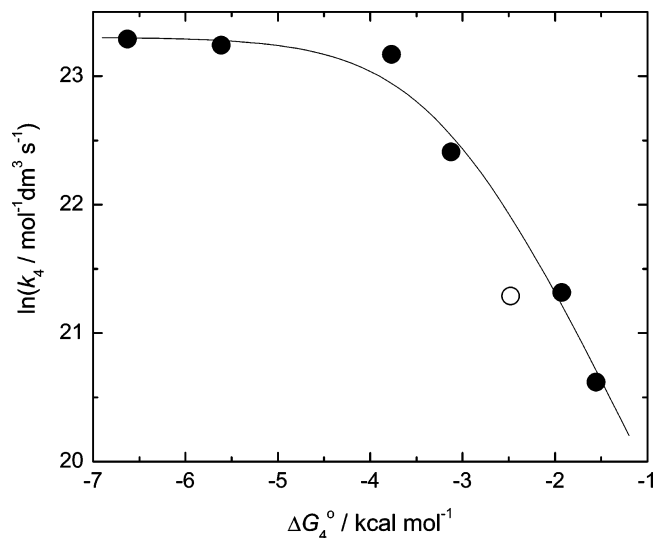


Figure 6. Plot of $\ln k_4$ as a function of the Gibbs energy change in the complexation reaction of ${}^1\mathbf{I}$ (i.e., ΔG_4°). The full line is calculated by using eq 15 (see text).

uncertainties are reflected by the statistical errors of rate coefficients given in the table.

In the above derivation of the rate coefficients, the assumption of irreversible complex formation is a critical question. Therefore, the validation of this assumption is required. If complex formation is reversible, we have a two-state system with kinetics similar to that of reversible exciplex formation. Using the known equations for such systems,¹⁷ the rate coefficients k_4 , k_{-4} , and $(k_9 + k_{10}[\mathbf{X}])$ can be derived from τ_0 , τ_1 , τ_2 , and A_2/A_1 (determined at the wavelength where only ${}^1\mathbf{I}$ emits). Such considerations have been made using experimental data for the \mathbf{I} -IPA-*n*-hexane system where ΔG_4° is the least negative. Since for this system the A_2/A_1 ratio cannot be determined with sufficient accuracy, we followed a different route. An iterative process has been used to find the A_2/A_1 ratio which yields (by the use of the appropriate equations¹⁷) the k_4 and k_{-4} rate coefficients which are in accordance with the $K_4 = k_4/k_{-4}$ equilibrium constant (derived from ΔG_4°). Using this A_2/A_1 ratio and the experimentally determined decay parameters, a rate coefficient of $k_4 = (9.5 \pm 0.3) \times 10^8 \text{ mol}^{-1} \text{ dm}^3 \text{ s}^{-1}$ is obtained. This is in excellent agreement with the rate coefficient $k_4 = (9.4 \pm 0.3) \times 10^8 \text{ mol}^{-1} \text{ dm}^3 \text{ s}^{-1}$ derived by assuming irreversible complexation.

5. Kinetics of Complexation Reactions. Analysis of the kinetic data presented in Table 1 shows that the rate coefficients of the two complexation processes 4 and 10 are very similar and the rate parameters decrease with decreasing hydrogen-bond-donating character of the alcohol (for which α_2^{H} is a measure). With alcohols of the highest hydrogen-bonding ability (i.e., TFE, HFIP, and PFTB), a diffusion-controlled rate was observed. This means that, in *n*-hexane, the activation-controlled process changes to a diffusion-controlled process at around $\Delta G^\circ = -4 \text{ kcal mol}^{-1}$. (Diffusion-controlled hydrogen-bonded-complex formation in the excited state was observed also by Inoue and co-workers⁷ for the aminoanthraquinone-ethanol systems in benzene and by Mataga et al.¹⁸ for the 1-aminopyrene/1-pyrenol-pyridine/methyl substituted pyridine systems in *n*-hexane.)

In the case of reaction 4, the dependence of the rate of complexation on the hydrogen-bonding ability of the alcohol was studied in detail. In Figure 6, the logarithm of k_4 is plotted against ΔG_4° , the Gibbs energy change in the complexation process of excited \mathbf{I} . The covered ΔG_4° range includes results

showing diffusion-controlled kinetics as well as data obtained in the transition region between diffusion-controlled and activation-controlled kinetics. To account for the observed dependence of k_4 on ΔG_4° , we express the rate coefficient of complexation of $^1\mathbf{I}$ with alcohols by means of the well-known expression:¹⁹

$$k_4 = \frac{k_{\text{diff}} k_{\text{act}}}{k_{\text{diff}} + k_{\text{act}}} \quad (13)$$

where k_{diff} and k_{act} are the rate coefficients for the diffusion-controlled and activation-controlled processes, respectively. As a first approximation, the activation Gibbs energy of the activation-controlled process (ΔG_4^\ddagger) may be estimated by using a linear free energy relationship

$$\Delta G_4^\ddagger = \gamma' + \delta' \Delta G_4^\circ \quad (14)$$

where γ' and δ' are constants. With this approximation,

$$k_4 = \frac{k_{\text{diff}}}{[1 + k_{\text{diff}}/\{\gamma \exp(-\delta \Delta G_4^\circ)\}]} \quad (15)$$

where $\gamma = \exp(-\gamma'/RT)$ and $\delta = \delta'/RT$. The experimental data given in Figure 6 were fitted with eq 15. (In the fitting, the experimental point for complexation with methanol was omitted, since it is not in agreement with the rest of the data for the homologous series. Anomalous behavior has been observed⁹ also in another complexation reaction of methanol in *n*-hexane.) The optimized parameters used to calculate the full line are $k_{\text{diff}} = 1.32 \times 10^{10} \text{ mol}^{-1} \text{ dm}^3 \text{ s}^{-1}$, $\gamma = 1.01 \times 10^8 \text{ mol}^{-1} \text{ dm}^3 \text{ s}^{-1}$, and $\delta = -1.52$. The optimized k_{diff} value is somewhat less than the value calculated from the Einstein–Stokes equation ($k_{\text{diff}} = 2 \times 10^{10} \text{ mol}^{-1} \text{ dm}^3 \text{ s}^{-1}$);²⁰ however, it is in excellent agreement with other experimental determinations.^{18a,20}

Equation 15 with the optimized parameters, derived for the complexation of the excited $^1\mathbf{I}$ species, can be used²¹ to estimate the rate coefficient of the complexation of the ground-state \mathbf{I} with alcohols (k_1), since the appropriate ΔG_1° values are available from the measured K_1 equilibrium constants. The estimation of such ground-state complexation rate coefficients is particularly important, since no good method is available for their experimental determination. As an example, we calculate from eq 15, with the known value of $\Delta G_1^\circ = -2.10 \text{ kcal mol}^{-1}$, $k_1 = 2.1 \times 10^9 \text{ mol}^{-1} \text{ dm}^3 \text{ s}^{-1}$, the rate coefficient of the complexation of \mathbf{I} with HFIP in *n*-hexane. Moreover, with $K_1 = 35 \text{ mol}^{-1} \text{ dm}^3$, $k_{-1} = 5.2 \times 10^7 \text{ s}^{-1}$ is obtained. In comparison with the diffusion-controlled complexation rate of $^1\mathbf{I}$ with HFIP (i.e., $k_4 = 1.24 \times 10^{10} \text{ mol}^{-1} \text{ dm}^3 \text{ s}^{-1}$), the corresponding ground-state value (k_1) is lower by a factor of about 6.

6. First Order Reactions Depopulating the Singlet Excited \mathbf{IX} State. The first order decay rate coefficient of $^1\mathbf{IX}$ (i.e., k_9), given in the eighth column of Table 1, seems to be significantly higher than that of $^1\mathbf{I}$ (i.e., $k_0 = 4.31 \times 10^7 \text{ s}^{-1}$). The rate coefficient k_9 is a composite quantity, the sum of the rate coefficients for fluorescence emission, singlet–triplet transition (ISC), and internal conversion (IC) from the singlet excited state of \mathbf{IX} :



Experimental fluorescence quantum yield and triplet yield values are available for the most studied \mathbf{I} –HFIP–*n*-hexane

system: $\Phi_f'(\mathbf{IX}) = 0.028 \pm 0.005$ and $\Phi_{\text{isc}}'(\mathbf{IX}) = 0.008 \pm 0.004$ at $[\text{HFIP}] = 0.01 \text{ mol dm}^{-3}$. It is to be noted that the experimentally measured fluorescence and intersystem crossing yields depend on the alcohol concentration as a result of the $^1\mathbf{IX}$ -consuming bimolecular reaction 10. These experimentally measured yields are denoted by $\Phi_f'(\mathbf{IX})$ and $\Phi_{\text{isc}}'(\mathbf{IX})$ in order to distinguish them from the hypothetical yields $\Phi_f(\mathbf{IX})$ and $\Phi_{\text{isc}}(\mathbf{IX})$ corresponding to zero alcohol concentration. The latter values are obtained from the experimentally determined fluorescence and intersystem crossing yields, respectively, by multiplying these with the τ_2^0/τ_2 ratio, where τ_2 and $\tau_2^0 = k_9^{-1}$ are the decay parameters determined at the given alcohol concentration and referring to zero alcohol concentration, respectively. Next, with $\Phi_f(\mathbf{IX})$ and $\Phi_{\text{isc}}(\mathbf{IX})$, the quantum yield of internal conversion is calculated: $\Phi_{\text{ic}}(\mathbf{IX}) = 0.94 \pm 0.02$. Finally, from the quantum yields and the τ_2^0 value, the rate coefficients for the first order reactions depopulating the singlet excited \mathbf{IX} state are obtained: $k_{9a} = 8.5 \times 10^6 \text{ s}^{-1}$, $k_{9b} = 2.4 \times 10^6 \text{ s}^{-1}$, and $k_{9c} = 1.6 \times 10^8 \text{ s}^{-1}$. A comparison of the kinetic results for the first order reactions of the excited \mathbf{I} and \mathbf{IX} species shows that complexation with the alcohol increases by almost 1 order of magnitude the rate of internal conversion to the ground state and makes IC the dominant decay process of $^1\mathbf{IX}$. Moreover, hydrogen bonding with the alcohol has no significant effect on the fluorescence and intersystem crossing rates under the experimental conditions studied.

The k_9 rate coefficients show a decrease of about 1 order of magnitude with increasing hydrogen-bonding ability of the alcohol. Analysis of these data reveals that the decreasing tendency of k_9 parallels the increase of the ionization energy (IE) of the complexing alcohol (see the last column of Table 1). This is in agreement with our conclusion (derived above) that IC is the dominating process of the first order depopulation of singlet excited \mathbf{IX} provided that electron transfer in the $^1\mathbf{IX}$ complex is of importance in determining the rate of internal conversion. Various possibilities may be considered for the detailed mechanism of IC including “excited-state quenching via unsuccessful electron transfer”,²² “acceleration of internal conversion by photochemical reactions”,²³ or “displacement of the hydrogen-bonded proton with consequent oscillations” leading to a quenching ground-state configuration.²⁴ Potential energy calculation may help to reveal the mechanism.

The temperature dependence of k_9 has been studied for the \mathbf{I} –isopropanol–*n*-hexane system in the temperature range 0–50 °C. The concentration of the isopropyl alcohol was 0.104 mol dm⁻³. From these measurements, a rate coefficient expression of $k_9 = (1.2 \pm 0.2) \times 10^{14} \exp\{-6.6 \pm 0.3 \text{ kcal mol}^{-1}/RT\} \text{ s}^{-1}$ is derived. The obtained Arrhenius parameters are in accordance with the conclusion that the dominating first order decay process of $^1\mathbf{IX}$ is internal conversion to the ground state probably via potential energy surface crossing. In the femto-second–picosecond time-resolved transient absorption study of the 1-aminopyrene–pyridine hydrogen-bonded complex in *n*-hexane, Mataga and co-workers¹⁸ observed the formation of an electron transfer (ET) state from the locally excited one. They stated that, after the formation of the ET state, a rapid proton movement takes place which induces destabilization of the ground state, leading to ultrafast internal conversion. If a similar mechanism applies for our studied system, the electron transfer state is expected to lie 6–7 kcal mol⁻¹ higher than $^1\mathbf{IX}$ (note the 6.6 kcal mol⁻¹ activation energy of reaction 9).

Acknowledgment. This work was supported by the Hungarian Science Foundation (OTKA T45890 and T043601).

References and Notes

- (1) Demeter, A.; Biczók, L.; Bérces, T.; Wintgens, V.; Valat, P.; Kossanyi, J. *J. Phys. Chem.* **1996**, *100*, 2001.
- (2) Demeter, A.; Bérces, T.; Zachariasse, K. A. *J. Phys. Chem. A* **2001**, *105*, 4611.
- (3) Cagniant, P.; Cagniant, D. *Adv. Heterocycl. Chem.* **1975**, *18*, 343. Reboledo, F. J.; Treus, M.; Estevez, J. C.; Castedo, L.; Estevez, R. *J. Synth. Lett.* **2003**, *11*, 1603 and references therein.
- (4) Herbich, J.; Hung, C.-Y.; Thummel, R. P.; Waluk, J. *J. Am. Chem. Soc.* **1996**, *118*, 3508. Waluk, J. *Acc. Chem. Res.* **2003**, *36*, 832 and references therein.
- (5) Vinogradov, S. N.; Linnell, R. H. *Hydrogen Bonding*; Van Nostrand Reinhold Company: New York, 1971.
- (6) Abraham, M. H. *Chem. Soc. Rev.* **1993**, *22*, 73. Abboud, J.-L. M.; Sraidi, K. Abraham, M. H.; Taft, R. W. *J. Org. Chem.* **1990**, *55*, 2230.
- (7) Yatsuhashi, T.; Inoue, H. *J. Phys. Chem. A* **1997**, *101*, 8166. Yatsuhashi, T.; Nakayima, Y.; Shimada, T.; Tachibana, H.; Inoue, H. *J. Phys. Chem. A* **1998**, *102*, 8657 and references therein.
- (8) Sebök-Nagy, K.; Biczók, L. *Photochem. Photobiol. Sci.* **2004**, *3*, 389. Biczók, L.; Bérces, T.; Linschitz, H. *J. Am. Chem. Soc.* **1997**, *119*, 11071.
- (9) Demeter, A.; Ravasz, L.; Bérces, T. *J. Phys. Chem. A* **2004**, *108*, 4357.
- (10) Demas, J. N.; Crossby, G. A. *J. Phys. Chem.* **1971**, *75*, 991.
- (11) Wintgens, V.; Valat, P.; Kossanyi, J.; Demeter, A.; Biczók, L.; Bérces, T. *J. Chem. Soc., Faraday Trans.* **1994**, *90*, 411.
- (12) Kanaoka, Y.; Koyama, K. *Tetrahedron Lett.* **1972**, *44*, 4517. Kanaoka, Y.; Koyama, K.; Hatanaka, Y. *J. Photochem.* **1985**, *28*, 575.
- (13) Disanayaka, B. W.; Weedon, A. C. *Can. J. Chem.* **1987**, *65*, 245.
- (14) Mataga, N. *Bull. Chem. Soc. Jpn.* **1957**, *30*, 375.
- (15) Adiabatic ionization energy obtained by photoelectron spectroscopy from NIST Chemistry WebBook, NIST Standard Reference Database Number 69, 2003 release, <http://webbook.nist.gov/chemistry/>.
- (16) This procedure was chosen in order to obtain the best estimate for the first excited singlet-state energy relative to the ground state. The absorption maximum at 360 nm belongs to a transition to a higher electronic state. Despite this, very similar results are obtained for Δ^1E , if the fluorescence maximum is adjusted to the maximum of the absorption band at 360 nm. This is because the shape of the absorption spectrum does not change considerably with complexation.
- (17) Il'ichev, Yu. V.; Kühnle, W.; Zachariasse, K. A. *J. Phys. Chem. A* **1998**, *102*, 5670. Rückert, I. *Photoinduzierter Elektronentransfer und interne Konversion*; Cuvillier Verlag: Göttingen, Germany, 1998; p 18.
- (18) Miyasaka, H.; Tabata, A.; Kamada, K.; Mataga, N. *J. Am. Chem. Soc.* **1993**, *115*, 7335. Miyasaka, H.; Tabata, A.; Ojima, S.; Ikeda, N.; Mataga, N. *J. Phys. Chem.* **1993**, *97*, 8222.
- (19) Pilling, M. J.; Seakins, P. W. *Reaction Kinetics*; Oxford University Press: Oxford, U.K., 1995; Chapter 6, p 143.
- (20) Atkins, P. W. *Physical Chemistry*, 4th ed.; Oxford University Press: Oxford, U.K., 1990; p 848.
- (21) This approximation is based on the assumption that **I** and **I** behave similarly with respect of complexation; however, they differ in the Gibbs free energy change of complexation (ΔG°) and consequently in the hydrogen-bond basicity (β_2^H).
- (22) Sinicropi, A.; Nau, W. M.; Olivucci, M. *Photochem. Photobiol. Sci.* **2002**, *1*, 537.
- (23) Plotnikov, V. G.; Maier, G. V. *Opt. Spectrosk.* **1979**, *47*, 62.
- (24) Our attention was drawn to this mechanism by one of the referees.